Bioorganic & Medicinal Chemistry 23 (2015) 3781–3787

Contents lists available at ScienceDirect

Bioorganic & Medicinal Chemistry

journal homepage: www.elsevier.com/locate/bmc

Synthesis and discovery of (I-3,II-3)-biacacetin as a novel non-zinc binding inhibitor of MMP-2 and MMP-9

Pandurangan Nanjan [†,‡], Jyotsna Nambiar [†,‡], Bipin G. Nair [‡], Asoke Banerji [*]

Amrita School of Biotechnology, Amrita Vishwa Vidyapeetham, Amrita University, Kollam, Kerala 690525, India

ARTICLE INFO

Article history:
Received 15 January 2015
Revised 29 March 2015
Accepted 31 March 2015
Available online 9 April 2015

Keywords:
Cerium ammonium nitrate (CAN)
(I-3,II-3)-Biflavones
Biacacetin
Non-zinc binding inhibitor
MMP-2 and MMP-9

ABSTRACT

Eleven biflavones (**7a**–**b** and **9a**–**i**) were synthesised by a simple and efficient protocol and screened for MMP-2 and MMP-9 inhibitory activities. Amongst them, a natural product-like analog, (I-3,II-3)-biacacetin (**9h**) was found to be the most potent inhibitor. Molecular docking studies suggest that unlike most of the known inhibitors, **9h** inhibits MMP-2 and MMP-9 through non-zinc binding interactions.

1. Introduction

(I-3,II-3)-Biflavones form a small group of dimeric flavonoids.[1] Due to limited occurrence and lack of convenient synthesis, this group of flavonoids have not been subjected to detailed bio-evaluation. Unlike synthetic strategies for C–O–C or C–C linked biflavones (e.g., Ullmann coupling and Suzuki reactions),[2] synthesis of (I-3,II-3)-biflavones has not been studied in detail.[3] During last three decades large numbers of inhibitors of matrix metalloproteinases (MMPs) have been identified but they lack selectivity due to the similarities in their active sites. Our earlier studies showed that anacardic acid inhibits MMP-2 and MMP-9 by interacting with the zinc in the catalytic site.[4] Recently non-zinc binding inhibitors are attracting attention due to their possible selectivity over MMPs.[5] With this in view, we screened eleven (I-3,II-3)-biflavones (**7a**–**b** and **9a**–**i**) for inhibition of MMP-2 and MMP-9 activities.

Oxidative dimerization of the flavones seems to be an attractive possibility for the synthesis of (I-3,II-3)-biflavones. Synthesis of (I-3,II-3)-hexamethyl biapigenin, **9e** by oxidative coupling of trimethyl apigenin using alkaline $K_3[Fe(CN)_6]$ has been described.[3a] But the yields of the reactions are very low due to side-reactions which makes the isolation process very cumbersome. Perusal of literature suggests that the use of CAN (ceric ammonium nitrate) could be a good option for dimerization of flavones through C–C oxidative coupling by a single electron transfer mechanism.[6] However, reaction of flavone **4a** with CAN under different reaction conditions did not yield biflavone **2** (Scheme 1). A retrosynthetic analysis (Fig. 1) suggests that a tetraketone intermediate (II, Fig. 1) obtainable from appropriately placed *o*-OH functionality in 1,3-diketone (I, Fig. 1) provides a good option for the synthesis of (I-3,II-3)-biflavones. Some examples of dimerization of 1,3-diketones to tetraketones by using Ag_2CO_3,[7] electrochemical[8] and CAN[9] reactions have been reported. To our knowledge, dimerization of diaryl-1,3-diketones have not been reported so far. The present article describes, development of a one pot synthesis of (I-3,II-3)-biflavones through the application of CAN mediated dimerization of appropriately substituted diaryl-1,3-diketones.

2. Results and discussion

2.1. Chemistry

The diaryl-1,3-diketones were conveniently synthesized by the Baker–Venkataraman transformation of appropriately substituted benzoyloxy esters of 2-hydroxyacetophenones as described earlier.[10] 1,3-Diketone **4** [1-(2-hydroxyphenyl)3-phenyl propane 1,3-dione)] did not undergo any change on treatment with CAN under various reaction conditions, and the starting material was recovered. We conjecture that this could be due to presence of the free *o*-hydroxyl group in **4**. Acetylation of **4** with acetic anhydride/pyridine gave **5** which on reaction with CAN at ambient

* Corresponding author. Tel.: +91 (476) 2801280; fax: +91 (476) 2899722.
E-mail address: banerjiasoke@gmail.com (A. Banerji).
† Equally contributed to this article.
‡ Tel.: +91 (476) 2801280; fax: +91 (476) 2899722.

http://dx.doi.org/10.1016/j.bmc.2015.03.084
0968-0896/

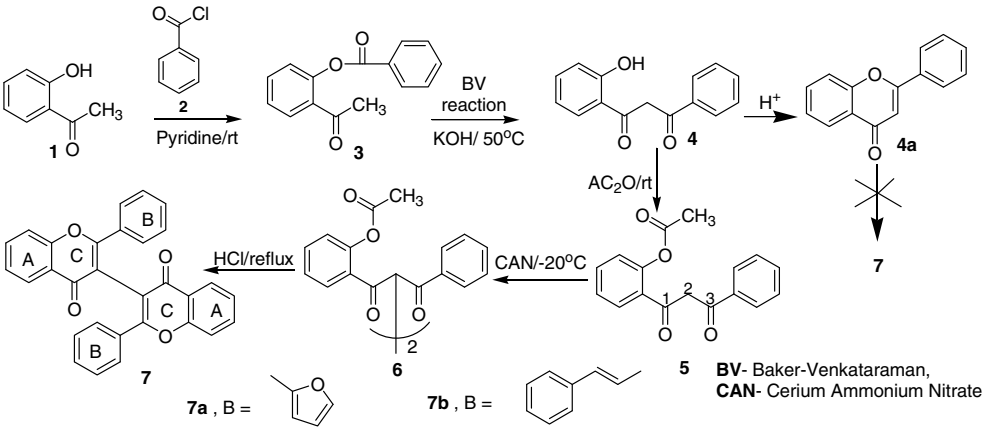

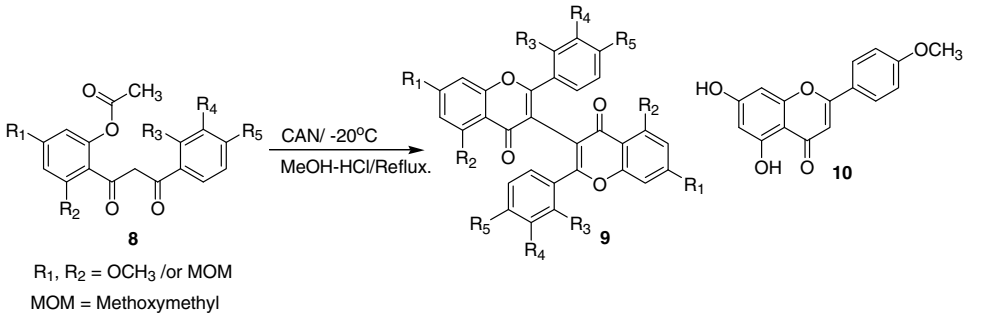

Entry	R_1	R_2	R_3	R_4	R_5	Yield (%)
9a	OCH_3	H	H	H	H	85
9b	H	H	OCH_3	H	H	88
9c	H	H	H	H	OCH_3	83
9d	OCH_3	OCH_3	H	H	H	82
9e	OCH_3	OCH_3	H	H	OCH_3	86
9f	OH	H	H	H	H	85
9g	OH	OH	H	H	H	83
9h	OH	OH	H	H	OCH_3	80
9i	OH	OH	H	OCH_3	OCH_3	78

Scheme 1. Synthesis of (I-3,II-3)-biflavones.

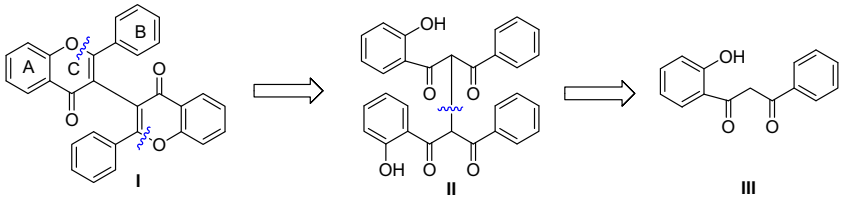

Figure 1. Retro-synthetic analysis of (I-3,II-3)-biflavones.

temperature gave the tetraketone **6** in 50% yield. The mass spectrum of **6** showed peak at *m*/*z* 563 $[M+H]^+$ corresponding to molecular formula, $C_{34}H_{26}O_8$ indicating successful dimerization of **5**. MS/MS of *m*/*z* 563 showed successive loss of two 60 units suggesting loss of two ketene (CH_2=C=O) units and two water (H_2O) molecules to give ion at *m*/*z* 443. Since **6** is a symmetrical dimer, only monomeric protons were observed in the ^{1}H NMR spectrum except that the methylene protons (2H) of **5** at δ 4.54 were replaced by the methine proton singlet (1H) at δ 6.71 in **6**, confirming that coupling reaction has occurred regiospecifically at 2-position (in structure **5**). Other features of MS, ^{1}H and ^{13}C NMR as well as IR and UV spectra were in complete agreement with the assigned structure **6**. When **6** was refluxed with 10% methanolic HCl (2 h), **7** was obtained in 78% yield. Biflavone **7** gave the expected molecular mass of *m*/*z* 443 $[M+H]^+$. MS/MS of *m*/*z* 443 ion showed successive loss of two fragments with mass unit 120, each giving ion at *m*/*z* 203. The loss of two 2′-hydroxy acetophenone moieties (2 × 120 units) arises from cleavage of two A rings. The mass spectral fragmentation along with the absence of singlet proton (δ 6.43)[10] at 3-position (corresponding to monomer, **10**) in ^{1}H NMR provide unequivocal evidence for the linkages of two flavone units through I-3 and II-3 positions. It is known that the CAN directed dimerization reactions are greatly influenced by the experimental factors such as solvents, temperature, etc. Therefore it was necessary to optimize the reaction conditions by conducting experiments using different solvent media and temperature (see Supplementary information). The best result for the dimerization of **5**–**6** (80–92% yield) was obtained using a mixture of MeCN/

MeOH/H_2O (1:1:1, v/v), CAN (1.1 equiv), at −20 °C for 30 min. Increasing the quantity of CAN did not improve the yield substantially. During the optimization of the protocol, it was observed that diketone **5** could be directly converted to biflavone **7** by adding CAN (1.1 equiv) under similar conditions (MeCN/MeOH/H_2O, −20 °C) followed by refluxing (2 h) in methanolic HCl (10%) without the isolation of tetraketone, **6**. Biflavone **7** was obtained with high yield (92%). Therefore, in subsequent experiments the diketones were directly transformed into biflavones in a one pot reaction. Scope of the reaction was further expanded by the preparation of **7a** (87%) and **7b** (84%) (Scheme 1). The generality of the protocol was established by taking differently substituted diketones. The methoxy diketones **8** were transformed into methoxybiflavones **9a**–**e** in good yields (Scheme 1). For the synthesis of polyhydroxy biflavones, it was necessary to protect the hydroxyl groups. MOM (methoxymethyl) group was preferred option for the protection of hydroxyl groups since it offers certain advantages over the conventional groups (e.g., benzyl, benzoyl) such as ease of preparation and regeneration of hydroxyl groups. The protected diketones were prepared using 4,6-diMOM phloroacetophenone, as described in our earlier publication.[10] The treatment of the diketones **8** with CAN, followed by methanolic–HCl (10%, 3 h) gave polyhydroxy and regiospecific partial methyl ethers of biflavones **9f**–**i** in good yield (Scheme 1). Deprotection of the MOM groups occurred during the final double cyclodehydration step. Thus, it was inferred that MOM and acetyl groups are compatible for the CAN mediated oxidative coupling.

2.2. Biological evaluation

In the present investigation, eleven different biflavones (**7a**–**b**, **9a**–**i**) were screened for their inhibition of MMP-2 and -9 activities in fibrosarcoma cells (HT1080). Amongst them, **9h** showed significant inhibition (90%) of both MMP-2 and -9 activities at a concentration of 10 μM (Fig. 2). Other compounds **9a**–**e** showed much less inhibition of gelatinases (data not shown). Dose-dependent inhibition of MMP-2 and -9 activities were observed when the cells were treated with different concentrations of **9h** (Fig. 3). These results were further confirmed using a fluorescent-based gelatin degradation assay which clearly shows the reduction in degradation of the gelatin at a concentration of 5 μM when compared to the control (Fig. 4). Analysis of the cytotoxicity of **9h** to HT1080 cells indicated that there was no significant toxicity up to a concentration of 7.5 μM (data not shown). The monomer of **9h**, that is, acacetin **10** did not show inhibition of MMP-2 and MMP-9 at a concentration of 5 μM (data not shown), whereas **9h** inhibits MMP-2 and MMP-9 by 60% and 90%, respectively, at this same concentration. This provides an evidence that the dimer **9h** is a better inhibitor of MMP-2 compared to its monomer. Since MMP-2 and MMP-9 are known to play a significant role in the migration of cancer cells, the effect of **9h** on cell migration was studied using transwell migration assay. **9h** showed reduction in migration of HT1080 cells from a concentration of 5 μM (Fig. 5).

2.3. SAR studies

Eleven variously substituted biflavones having hydroxy-, methoxy-, furano- and cinnamyl- moieties were evaluated for the inhibition of MMP-2 and MMP-9. While biacacetin (**9h**) showed maximum inhibition for both MMP-2 and MMP-9, other compounds showed differential activities. For example, biflavones **7a**, **9f** and **9i** showed significantly lower inhibitions for MMP-2 compared to **9h** (Fig. 2). Similarly methoxy derivatives (**9a**–**9e**) did not show significant inhibition of MMP-2 and MMP-9 (data not shown). The compounds which lack the hydroxyl in the position

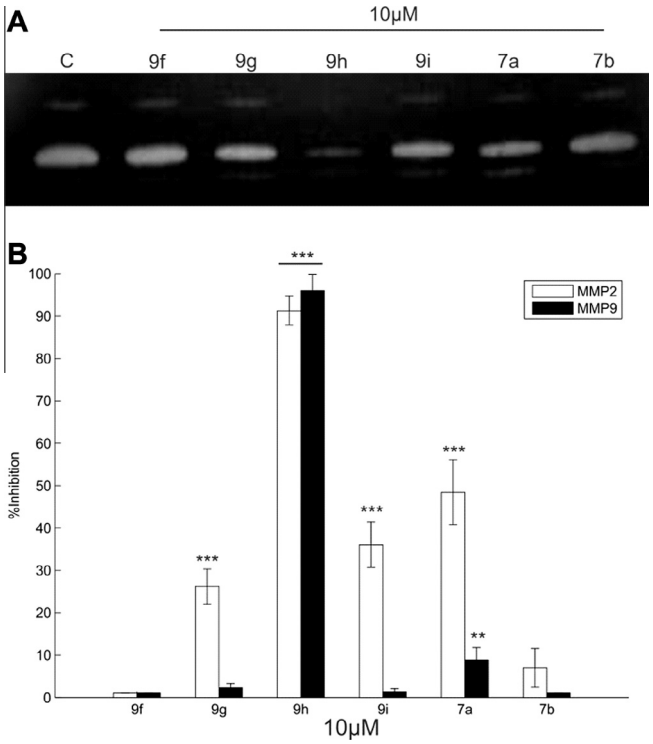

Figure 2. Regulation of MMP-2 and -9 (gelatinases) activity by (I-3,II-3)-biflavones. (A) Zymogram showing gelatinase activity of conditioned media from HT1080 cells treated with 0.5% DMSO (lane 1), 10 μM **9f**, **9g**, **9h**, **9i**, **7a**, **7b** (lanes 2–7, respectively). (B) A representative plot of percentage inhibition observed in the zymogram. Each bar represents the Mean ± SE of triplicate determinations from three independent experiments. ***P <0.001 (one-way analysis of variance with Dunnett's multiple-comparison post-test).

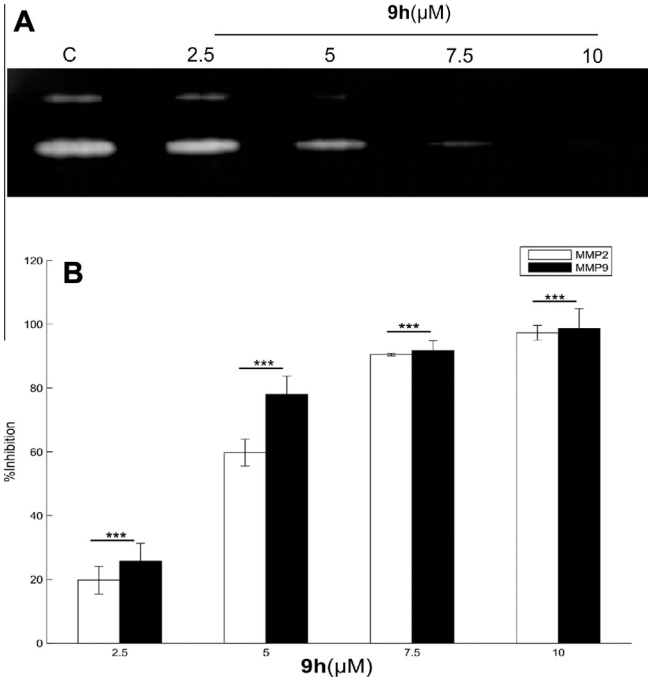

Figure 3. Dose dependent study of **9h**. (A) Zymogram showing gelatinase activity of conditioned media from HT1080 cells treated with 0.5% DMSO (lane 1) and 2.5, 5, 7.5 and 10 μM **9h** (lanes 2–5, respectively). (B) A representative plot of percentage inhibition observed in the zymogram. Each bar represents the Mean ± SE of triplicate determinations from three independent experiments. ***P <0.001 (one-way analysis of variance with Dunnett's multiple-comparison post-test).

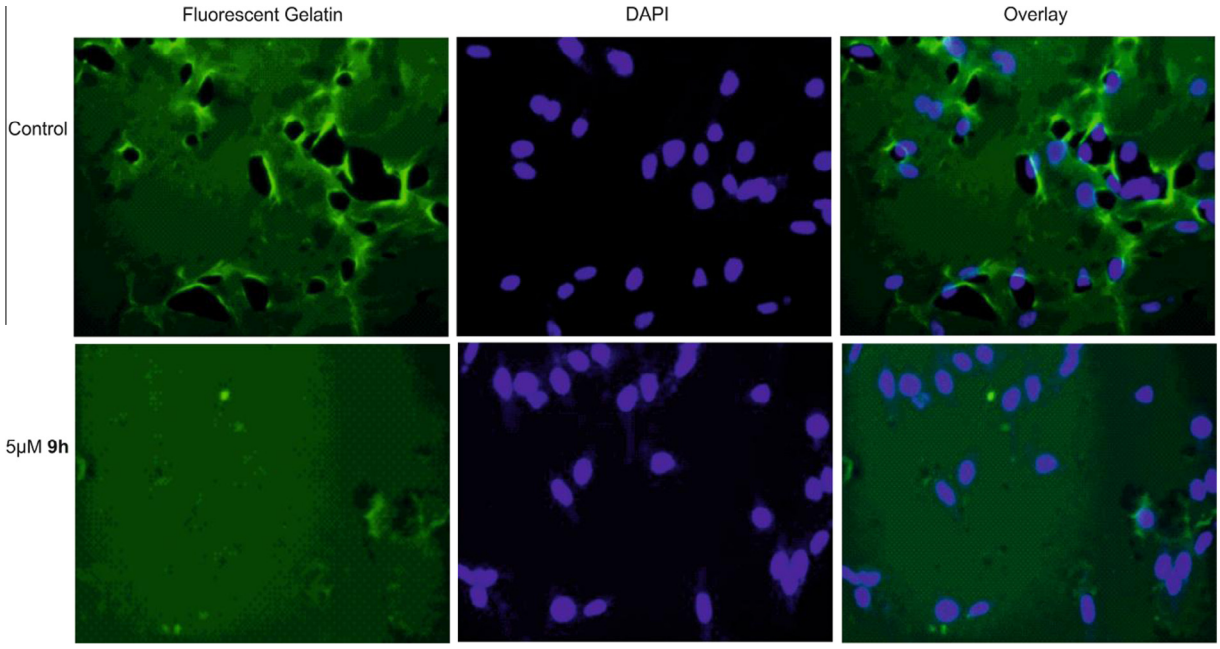

Figure 4. Regulation of gelatinase activity by **9h**. Gelatin degradation assay showing the reduction in degradation of the fluorescent gelatin at 5 μM **9h** when compared to control.

R2 (as in **9f** and **7b** in Scheme 1) did not show significant inhibition of MMP-2 and MMP-9.

2.4. Molecular docking

Active sites of most of the MMPs are conserved and result in lack of selectivity in inhibition.[5,11] Amongst the biflavones (**7a**–**b** and **9a**–**i**) tested, **9h** was found to be the most potent inhibitor of MMP-2 and -9. Molecular dynamic simulation studies indicate that, while the S1′ pocket in MMP-2 is narrow, that of MMP-9 has a relatively larger pocket-like subsite.[5,11] To simulate the interaction of **9h** with the target proteins, 'Autodock'-based molecular modeling programme was used. The parameters for docking were fixed on the basis of our previously published work.[4] **9h** forms four hydrogen bonds with MMP-2 catalytic domain [(PDB code—1QIB) (docking score; −7.6)]; one between 7-OH (I) and Thr229, while the other three are between Arg119 and 5-OH (I), 4-(I) and 4(II) carbonyls (Fig. 6A, Supplementary Fig. 1). **9h** also forms hydrophobic interactions with Phe196, Phe232, Leu197 and Gln122. It is noteworthy that unlike most of the MMP inhibitors such as anacardic acid (Supplementary Fig. 2) and batimastat, **9h** does not bind to the zinc in the catalytic site. A probable explanation could be the larger size and rigid nature of **9h** that results in reduced accessibility to the active site of MMP-2 (deeper S1′ tunnel). **9h** binds in a region between α-helix and S1′ specificity loop (indicated in Fig. 6A). The MMP-9 catalytic domain [(PDB code—2OVX) (docking score; −7.5)] was also subjected to docking study. **9h** did not show any hydrogen bonding with MMP-9; it exhibited only hydrophobic interactions with the amino acid residues (Phe110, Leu187, His401, His405, His411 and Pro421) (Supplementary Fig. 3). The lengthy S1′ sub-site in MMP-9 precludes the interaction of **9h** with S1′ site and hence prevents interaction of **9h** with the zinc (Fig. 6B). **9h** was also compared with its monomer **10** with respect to its binding (data not shown). Although **10**, exhibited interaction at the active site (zinc) in both MMP-2 and MMP-9, inhibition of MMP-2 activity was significantly reduced. We report here for the first time that this natural product like analog, (I-3,II-3)-biacacetin is a novel *non-zinc binding inhibitor* for MMP-2 and -9. The non-zinc-binding inhibitory activity of this molecule is under further studied for selectivity and specificity of the different MMPs.

3. Conclusion

In conclusion, a new synthesis of (I-3,II-3)-biflavones through oxidative dimerization of poly-substituted diaryl-1,3-diketones with cerium ammonium nitrate followed by double cyclodehydration has been developed. A systematic screening of biflavones (**7a**–**b**, **9a**–**i**) for inhibition of MMP-2 and -9 was carried out; **9h** was found to be best inhibitor. In silico docking studies suggests that (I-3,II-3)-biacacetin inhibits the gelatinases through non-zinc binding interactions. The non-zinc binding nature of (I-3,II-3)-biacacetin could be an important factor for designing selective molecules of therapeutic importance through inhibition of MMP-2 and MMP-9.

4. Experimental

4.1. Chemistry

4.1.1. Preparation of tetraketone 6

To **5** (1 mmol) in methanol (4 ml) at 28 °C, Ceric ammonium nitrate (1 mmol, in 1 ml methanol) was added and stirred for 12 h. (monitored by TLC; toluene 5: methanol 5: formic acid 2), methanol was removed under reduced pressure, water (10 ml) was added, then extracted with dichloromethane (10 ml × 2), dried over anhydrous Na_2SO_4. Solvent removed and white solid was obtained. After column chromatography, product **6** was obtained. **6** were characterized by ^{1}H NMR, ^{13}C NMR, MASS, IR, UV spectral and HPLC analysis.

4.1.2. Deprotection and cyclodehydration of 6 (preparation of 7)

To **6** (1 mmol), methanolic–HCl (20 ml, 10%) was added and refluxed for 2 h. After monitoring by TLC, solvent was removed under reduced pressure. Water added to the reaction mass, extracted with ethyl acetate (10 ml × 2). Washed with water (5 ml × 2), dried with anhydrous Na_2SO_4. Solvent removed and

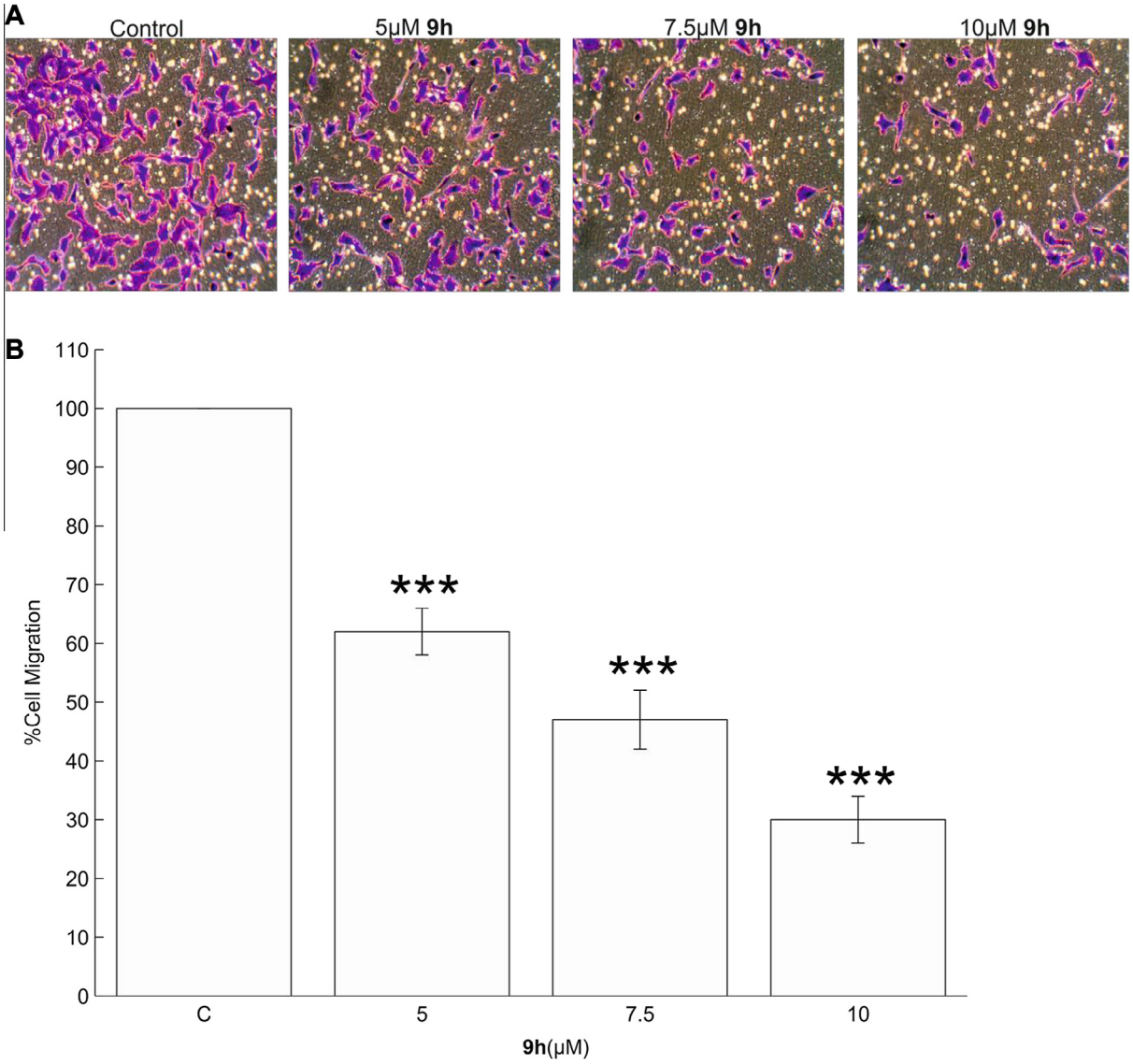

Figure 5. Effects of **9h** on migration of HT1080 cells. (A) The cells were treated with different concentrations of **9h** in serum-free medium and DMEM with 10% FBS was used as the attractant. After 24 h of culture, the cells that migrated through the pores were stained and photographed under microscope. (B) The graph displays percentage of cells migrated with respect to control in five random fields. Each bar represents the Mean ± SE of the number of cells obtained in the five random fields. ***P <0.001 (one-way analysis of variance with Dunnett's multiple-comparison post-test).

white solid was obtained. The overall conversion **5**–**7**, via tetraketone **6** was 39%. The (I-3, II-3)-biflavone crystallized with methanol-chloroform mixture. Characterization of **7** is given below.

4.1.3. General procedure for the conversion of 1,3-diketones to (I-3,II-3)-biflavones; one pot synthesis of (I-3,II-3)-biflavones (7–7b and 9a–9j)

Acetate protected 1,3-diketones (1 mmol) were taken in MeCN/MeOH (1:1, 8 ml). CAN (1.1 equiv in water 4 ml) was added to the reaction mixture at −20 °C over 5 min. Then reaction mixture was stirred for 30 min; after monitoring (TLC) methanolic–HCl (10%, 30 ml) was added and refluxed for 2–3 h. After that, solvent was removed; water was added and extracted with ethyl acetate (20 ml × 2). Washed well with water (5 ml × 2), dried over anhydrous Na_2SO_4. Fast column chromatography was performed using SiO_2. Biflavones were obtained in good yield: 78–92% directly without isolating tetraketones. Characterizations of all biflavones are given below.

4.1.3.1. Characterization of 6. Tetraketone **6** was obtained as colorless needles. Mp 150–151 °C. UV λ_{max} (MeOH)/nm; 250. IR ν_{max}/cm^{-1}; 1761 (CO) and 1687 (CO). ^{1}H NMR (400 MHz, DMSO-d_6); δ 7.94, m, 2H; 7.6, m, 1H; 7.53, m, 1H; 7.45, t, 2H; 7.32, t, 2H; 7.09, dd, 1H; 6.71, s, 1H; 2.26, s, 3H. ^{13}C NMR (100 MHz, DMSO-d_6); 193.84, 193.68, 168.65, 148.11, 135.75, 134.03, 133.9, 130.01, 129.97, 128.71, 126.23, 124.06, 59.94 and 20.66. LC–MS; Rt-16.133, Purity-97%, $[M+1]^+$ = 563, MS/MS = 503, 443.

4.1.3.2. Characterization of 7. **7** was obtained as colorless crystals. Mp 330–332 °C. UV λ_{max} (MeOH)/nm; 254 and 310. IR ν_{max}/cm^{-1}; 1643 (CO). ^{1}H NMR (400 MHz, DMSO-d_6): δ 8.12, m, 1H; 7.9, m, 1H; 7.72, d (J = 8.0 Hz), 1H; 7.59, m, 1H; 7.42, m, 1H; 7.36, t, 2H; 7.22, t, 2H. ^{13}C NMR (100 MHz, DMSO-d_6): 176.01, 162.64, 155.59, 134.7, 132.2, 130.69, 128.44, 127.36, 125.87, 125.35, 121.92 and 118.47. LC–MS: Rt-15.848, Purity-95% $[M+1]^+$ = 443, MS/MS = 323, 203.

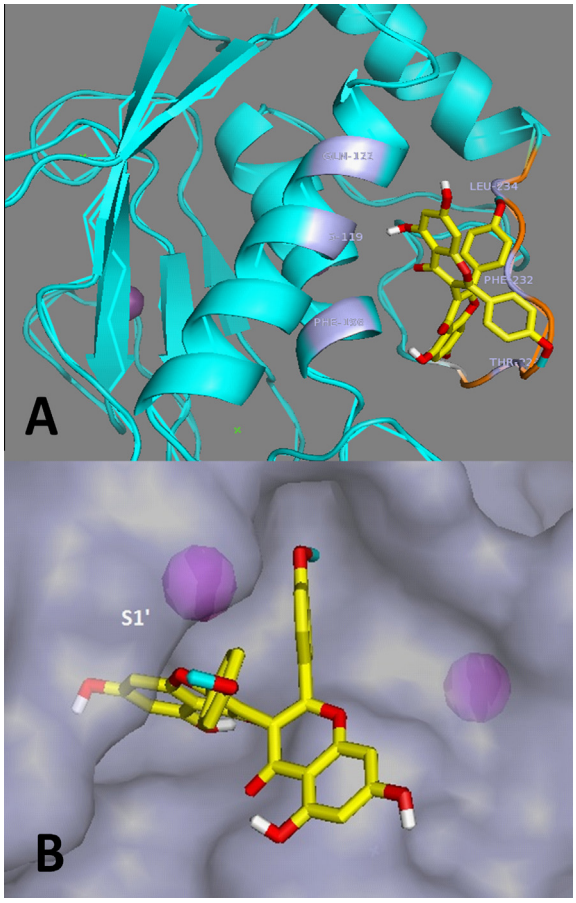

Figure 6. Predicted binding mode of **9h** to MMP-2 and MMP-9. (A) Ligand **9h** (stick model, carbon-yellow, red-oxygen, hydrogen-white and methyl group-cyan color) interaction with MMP-2 catalytic domain (violet sphere-zinc metal, Orange-S1′ specificity loop, light blue-interaction of amino acid residues with the ligand). (B) Surface structure of MMP-9 with **9h**. Surface structure shows that **9h** binds outside the S1′ active site.

4.1.3.3. Characterization of 7a. **7a** was obtained as yellow crystals. Mp 200–202 °C. UV λ_{max} (MeOH)/nm; 247 and 314. IR ν_{max}/cm^{-1}; 1641 (CO). ^{1}H NMR (400 MHz, DMSO-d_6): δ 8.11, m, 1H; 8.02, m, 1H; 7.93, d (J = 8.0 Hz), 1H; 7.9, m, 1H; 7.85, d (J = 16.0 Hz), 1H; 7.77, d, (J = 8.4 Hz), 1H: 7.61, d (J = 36.0 Hz), 7.59, m, 1H: 7.55, m, 1H: 7.06, m, 2H: 6.8, m, 1H. ^{13}C NMR (100 MHz, DMSO-d_6): 176.09, 174.77, 155.24, 154.83, 154.45, 153.5, 148.56, 147.53, 145.01, 144.87, 134.96, 134.37, 126.03, 125.59, 125.3, 124.84, 123.57, 122.37, 118.36, 118.19, 117.12, 115.64, 115.39, 112.9, 109.08 and 104.56. LC–MS: Rt-15.491, Purity-97.5%, $[M+1]^+$ = 423, MS/MS = 303, 183.

4.1.3.4. Characterization of 7b. **7b** was obtained as yellow crystals. Mp 269–272 °C. UV λ_{max} (MeOH)/nm; 259 and 337. IR ν_{max}/cm^{-1}; 1622 (CO). ^{1}H NMR (400 MHz, DMSO-d_6): δ 7.99, m, 1H; 7.85, m, 1H; 7.7, m, 2H; 7.59, m, 2H; 7.45, m, 1H; 7.28, m, 3H: 6.94, d (J = 16.0 Hz). ^{13}C NMR (100 MHz, DMSO-d_6): 175.76, 159.93, 155.32, 137.49, 134.94, 134.24, 129.8, 128.81, 128.12, 125.21, 125.14, 122.8, 119.03, 118.21 and 114.17. LC–MS: Rt-15.335, Purity-94.5%, $[M+1]^+$ = 503, MS/MS = 383, 263.

4.1.3.5. Characterization of 9a. **9a** was obtained as colorless crystals. Mp 238–241 °C. UV λ_{max} (MeOH)/nm; 244 and 306. IR ν_{max}/cm^{-1}; 1635 (CO). ^{1}H NMR (400 MHz, DMSO-d_6): δ 8.0, d (J = 8.8 Hz), 1H; 7.44, m, 1H; 7.34, m, 2H; 7.2, m, 3H; 7.13, dd, 1H; 3.91, s, 3H. ^{13}C NMR (100 MHz, DMSO-d_6): 175.38, 164.15, 162, 157.43, 132.28, 130.53, 128.35, 127.30, 126.78, 115.81, 115.73, 115.18, 100.71 and 56.16. LC–MS: Rt-6.722, Purity-96%, $[M+1]^+$ = 503, MS/MS = 488, 369, 235.

4.1.3.6. Characterization of 9b. **9b** was obtained as dull white crystals. Mp 257 °C (dec). UV λ_{max} (MeOH)/nm; 243 and 308. IR ν_{max}/cm^{-1}; 1631 (CO). ^{1}H NMR (400 MHz, DMSO-d_6): δ 8.16, m, 1H; 7.9, m, 1H; 7.83, m, 2H; 7.54, m, 1H; 7.4, m, 1H; 6.94, d, (J = 8.4 Hz), 1H: 6.81, m, 2H: 3.61, s, 3H. ^{13}C NMR (100 MHz, DMSO-d_6): 175.94, 156.43, 155.66, 134.27, 131.9, 129.01, 125.47, 125.19, 122.23, 120.73, 119.87, 118.24, 118.06, 111.27 and 55.03. LC–MS: Rt-5.456, Purity-97%, $[M+1]^+$ = 503, MS/MS = 488, 383, 263.

4.1.3.7. Characterization of 9c. **9c** was obtained as yellow crystals. Mp 248–249 °C. UV λ_{max} (MeOH)/nm; 269 and 307. IR ν_{max}/cm^{-1}; 1685 (CO). ^{1}H NMR (400 MHz, DMSO-d_6): δ 7.90, d (J = 8.8 Hz), 2H; 7.59, d (J = 2.4 Hz), 1H; 7.3, t, 1H; 7.2, t, 2H; 7.10, d (J = 8.8 Hz), 2H; 7.02, dd, 1H; 3.82, s, 3H. ^{13}C NMR (100 MHz, DMSO-d_6): 175.38, 166.95, 162.82, 132.28, 131.3, 122.96, 115.81, 115.72, 115.18, 100.71 and 55.4. LC–MS: Rt-6.551, Purity-96.5%, $[M+1]^+$ = 503, MS/MS = 488, 383, 263.

4.1.3.8. Characterization of 9d. **9d** was obtained as white crystals. Mp 175–178 °C. UV λ_{max} (MeOH)/nm; 269 and 303. IR ν_{max}/cm^{-1}; 1628 (CO). ^{1}H NMR (400 MHz, DMSO-d_6): δ 8.05, dd, 2H; 7.58, m, 3H; 6.88, d (J = 2.4), 1H; 6.52, d (J = 2.4), 1H. 3.90, s, 3H; 3.64, s, 3H. ^{13}C NMR (100 MHz, DMSO-d_6): 143.98, 139.26, 129.29, 123,116.1, 116.7, 116.8, 95.2, 80.25, 60.32 and 55.4. LC–MS: Rt-16.563, Purity-98%, $[M+1]^+$ = 563, MS/MS = 381, 199.

4.1.3.9. Characterization of 9e. **9e** was obtained as colorless crystals. Mp 190 °C (dec).[3a] UV λ_{max} (MeOH)/nm; 265 and 310. IR ν_{max}/cm^{-1}; 1622 (CO). ^{1}H NMR (400 MHz, DMSO-d_6): δ 7.22, d (J = 8.8 Hz), 2H; 6.89, d (J = 8.8 Hz), 2H; 6.72, s, 1H; 6.52, s, 1H; 3.88, s, 3H; 3.82, s, 3H; 3.74, s, 3H. ^{13}C NMR (100 MHz, DMSO-d_6): 162.15, 128.88, 113.78, 111.72, 109.49, 103.84, 103.76, 56.61 and 55.13. LC–MS: Rt-17.362, Purity-96%, $[M+1]^+$ = 623, MS/MS = 608, 441, 259.

4.1.3.10. Characterization of 9f. **9f** was obtained as pale yellow needles. Mp 220 °C (dec). UV λ_{max} (MeOH)/nm; 249 and 308. IR ν_{max}/cm^{-1}; 1627 (CO). ^{1}H NMR (400 MHz, DMSO-d_6): δ 10.8, s, 1H; 8.07, dd, 2H; 7.91, d (J = 8.8 Hz), 1H; 7.59, m, 3H; 7.01, d (J = 2.4 Hz), 1H; 6.99, dd, 1H; 6.95, d (J = 2.4 Hz), 1H. ^{13}C NMR (100 MHz, DMSO-d_6): 176.37, 162.75, 161.95, 157.5, 131.51, 131, 130, 129.06, 126.52, 126.15, 116.16, 115.06, 106.63 and 102.54. LC–MS: Rt-4.765, Purity-97%, $[M+1]^+$ = 475, MS/MS = 355, 219.

4.1.3.11. Characterization of 9g. **9g** was obtained as pale yellow solid. Mp 228–230 °C. UV λ_{max} (MeOH)/nm; 269 and 306. IR ν_{max}/cm^{-1}; 1638 (CO). ^{1}H NMR (400 MHz, DMSO-d_6): δ 7.27, d (J = 8.8 Hz), 1H; 6.88, d, (J = 8.8 Hz), 1H: 6.38, d (J = 2.0 Hz), 1H: 6.19, d (J = 8.0 Hz), 1H. ^{13}C NMR (100 MHz, DMSO-d_6): 181.85, 164.41, 163.87, 161.45, 157.45, 132, 130.71, 129.12, 126.4, 105.18, 103.96, 99.01 and 94.11. LC–MS: Rt-4.701, Purity-94%, $[M+1]^+$ = 507, MS/MS = 354, 201.

4.1.3.12. Characterization of 9h. **9h** was obtained as pale yellow solid. Mp 305 °C (dec). UV λ_{max} (MeOH)/nm; 270 and 333. IR ν_{max}/cm^{-1}; 1649 (CO). ^{1}H NMR (400 MHz, DMSO-d_6): δ 7.27, d

(J = 8.8 Hz), 1H; 6.88, d, (J = 8.8 Hz), 1H: 6.38, d (J = 2.0 Hz), 1H: 6.19, d (J = 8.0 Hz), 1H: 3.61, s, 3H. ^{13}C NMR (100 MHz, DMSO-d_6): 180.72, 164.71, 161.43, 161.28, 157.26, 129.26, 123.91, 114.13, 111.82, 98.96, 93.72 and 55.37. LC–MS: Rt-3.477, Purity-96%, $[M+1]^+$ = 567, MS/MS = 552, 414, 261.

4.1.3.13. Characterization of 9i. **9i** was obtained as yellow solid. Mp 263 °C (dec). UV λ_{max} (MeOH)/nm; 270 and 341. IR ν_{max}/cm^{-1}; 1651 (CO). ^{1}H NMR (400 MHz, DMSO-d_6): δ 12.91, s, 1H; 10.83, s, 1H; 7.69, dd, 1H: 7.56, d, (J = 2.0 Hz), 1H; 7.14, d (J = 8.4 Hz), 1H: 6.53, d (J = 4.8 Hz), 1H; 6.21, d, (J = 2.4 Hz), 1H; 3.88, s, 3H; 3.84, s, 3H. ^{13}C NMR (100 MHz, DMSO-d_6): 181.8, 164.18, 161.41, 157.35, 152.15, 149.02, 122.91, 120.04, 111.72, 109.42, 103.84, 103.76, 98.86, 94.09 and 55.73. LC–MS: Rt-5.273, Purity-98%, $[M+1]^+$ = 597, MS/MS = 444, 291.

4.2. Biological evaluation

4.2.1. Cell culture

HT1080 (human fibrosarcoma cells) were obtained from National Centre for Cell Sciences, Pune, Maharashtra, India. HT1080 cells were cultured in Dulbecco's modified Eagle's medium (DMEM) supplemented with 10% fetal bovine serum (v/v), 1% penicillin, 1% streptomycin, 0.1% amphotericin B (Sigma–Aldrich, St. Louis, MO). Fetal bovine serum (FBS) was purchased from Invitrogen (Carsbad, CA).

4.2.2. Gelatin Zymography

The zymography assay was performed according to the protocol described by Ratnikov et al.[12] Gelatin substrate gels were prepared by incorporating gelatin (2 mg/ml) into 10% polyacrylamide gel containing 0.4% SDS. Electrophoresis was carried out under non-reducing conditions at 120 V for 150 min. The gels were washed in 2.5% Triton X-100 (v/v) for 30 min and then incubated overnight at 37 °C in developing buffer containing 50 mM Tris–HCl, pH 7.6, 200 mM NaCl, 5 mM $CaCl_2$ and 0.2% (v/v) Brij-35. Digestion bands were quantified using BIORAD image analyzer systems.

4.2.3. Gelatin degradation assay

The assay was carried out according to the protocol described previously.[13] The cells were treated with 5 μM 9 h for 24 h at 37 °C. After treatment, the cells were fixed, mounted in ProLong® Gold Antifade reagent (Molecular probes, P-36931) and observed using IX71 Inverted microscope (Olympus).

4.2.4. Cell migration assay

HT1080 cells (8×10^4 cells) were treated with different concentrations of 9 h in 300 μL serum-free media and plated in the upper chamber. The lower chamber contained 750 μl of 10% serum-containing media. After 24 h of incubation, non-migratory cells in the upper chamber were carefully removed with a cotton swab. Migrated Cells were stained with crystal violet solution. The cell numbers were randomly counted in five fields.

4.3. Molecular docking

In order to identify the binding mode of the compound **9h**, AutoDockTools (http://mgltools.scripps.edu) was used. The crystal structure of MMP-2 catalytic domain (PDB code 1QIB) and MMP-9 catalytic domain (PDB code 2OVX) were obtained from RCSB PDB data bank. For docking studies, a grid box of 44 × 46 × 60 points on 0.375-Å grid spacing, centered on the ligand-binding sites for MMP-2 or MMP-9 identified by autoligand, were used to generate affinity maps. The best docking pose of **9h** was selected and analyzed. For validation, docking of **9h** was compared with anacardic acid.[4]

Acknowledgements

We would like to thank Mr. Muralidharan V (Amrita Agilent Analytical Research Lab) for acquiring the mass spectrometry data, Dr. Uday Singh (Sam Higginbottom Institute of Agriculture, Technology & Sciences, Deemed University, Allahabad, India) for his valuable suggestions on docking studies, Ms. Asha Vijayan and Mr. Krishna Chaitanya Medini for helping with Corel DRAW and MATLAB and University Grants Commission [F.2-7/2012(SA-I)] for providing financial assistance to Ms. Jyotsna Nambiar.

Supplementary data

Supplementary data associated with this article can be found, in the online version, at http://dx.doi.org/10.1016/j.bmc.2015.03.084.

References and notes

1. Daneel, F.; Desmond, S.; Jannie, P. J. M. In *Flavonoids Chemistry, Biochemistry and Applications*; Andersen, O. M., Markham, K. R., Eds.; Taylor & Francis: Broken Sound Parkway NW, Boca Raton, 2006; pp 1103–1112.
2. Rahman, M.; Riaz, M.; Desai, U. R. *Chem. Biodivers.* **2007**, *4*, 2495.
3. (a) Molyneux, R. J.; Wan, A. C.; Haddon, W. F. *Tetrahedron* **1969**, 1409; (b) Jieping, Z.; Qian, W.; Yulin, L. *J. Chem. Soc., Chem. Commun.* **1988**, 1549.
4. Athira, O.; Jyotsna, N.; Rodney, M. H.; Chinchu, B.; Pandurangan, N.; Rebu, K. V.; Geetha, B. K.; John, A. T.; Banerji, A.; Jefferson, P. P.; Bipin, G. N. *Mol. Pharm.* **2012**, *82*, 614.
5. (a) Jennifer, A. J.; Jody, L. M. J.; Melissa, T. M.; Seth, M. C. *Biochim. Biophys. Acta* **2010**, *1803*, 72; (b) Pizio, A. D.; Laghezza, A.; Tortorella, P.; Agamennone, M. *Chem. Med. Chem.* **2013**, 1.
6. (a) Nair, V.; Deepthi, A. *Chem. Rev.* **2007**, *107*, 1862; (b) Sridharan, V.; Menéndez, J. C. *Chem. Rev.* **2010**, *110*, 3805.
7. Hoing, B. C.; Shen, I. C.; Liao, J. H. *Tetrahedron Lett.* **2001**, *42*, 935.
8. Elinson, M. N.; Lizunova, T. L.; Nikishin, G. I. *Russ. Chem. Bull.* **1992**, *1*, 123.
9. Jianan, S.; Hao, Z.; Xianjun, C.; Xinsheng, L.; Dongcheng, X. *Synth. Commun.* **2010**, *40*, 1847.
10. Pandurangan, N. *Lett. Org. Chem.* **2014**, *11*, 225.
11. Nagase, H. In *Cancer Drug Discovery and Development: Matrix Metalloproteinase Inhibitors in Cancer Therapy*; Neil, J. C., Krzysztof, A., Eds.; Humana Press: Totowa, NJ, 2001; pp 33–66.
12. Mueller, S. C.; Chen, W. T. *J. Cell Sci.* **1991**, *99*, 213.
13. Ratnikov, B. I.; Deryugina, E. I.; Strongin, A. Y. *Lab. Invest.* **2002**, *82*, 1583.